Isospin mixing in the $T = 5/2$ ground state of ^{71}As

N. Severijns,[1] D. Vénos,[2] P. Schuurmans,[1] T. Phalet,[1] M. Honusek,[2] D. Srnka,[2] B. Vereecke,[1] S. Versyck,[1]
D. Zákoucký,[2] U. Köster,[3] M. Beck,[1] B. Delauré,[1] V. Golovko,[1] and I. Kraev[1]

[1]*Instituut voor Kern- en Stralingsfysica, K.U. Leuven, B-3001 Leuven, Belgium*
[2]*Nuclear Physics Institute, Acad. Sci. Czech Rep., CZ-25068 Rez, Czech Republic*
[3]*ISOLDE, CERN, CH-1211 Genève 23, Switzerland*

The presence of isospin mixing in the $T = 5/2$ ground state of ^{71}As was studied via anisotropic positron emission from oriented nuclei. A small isospin-forbidden Fermi component in the predominantly Gamow-Teller β decay was established, corresponding to an isospin mixing probability of $(13 \pm 4) \times 10^{-6}$. The sign of the magnetic moment of ^{71}As was determined to be positive.

I. INTRODUCTION

In recent years, the development of more powerful techniques for the production of exotic nuclei far from the line of stability has allowed the production of many new isotopes near the $N = Z$ line. Thus, all $N = Z$ isotopes up to the doubly magic ^{100}Sn and many neighboring isotopes are now accessible for decay studies [1–3]. This has also triggered renewed theoretical interest in this region, which is of special importance for the understanding of nuclear structure since protons and neutrons occupy the same orbitals here. One may thus expect near the $N = Z$ line a reinforcement of the proton-neutron pairing correlations, which are weak in nuclei close to the line of stability where the valence nucleons occupy different shells. A topic of particular interest for nuclei close to the $N = Z$ line is that of isospin impurities, i.e., the mixing of states with isospin $T \neq T_0$ into states with $T = T_0$. This phenomenon is predominantly caused by the Coulomb interaction but also by charge-dependent terms in the nucleon-nucleon interaction. In the $N \simeq Z$ region, this mixing is enhanced because of an increased overlap between the neutron and proton wave functions.

A good understanding of the mechanism of isospin mixing for nuclei in the $N = Z$ region is necessary in order to calculate reliable values for the isospin symmetry-breaking correction δ_C that is needed to extract the Fermi constant G_V from the $\mathcal{F}t$ values for superallowed Fermi β decays. Recently, new theoretical and experimental results have become available for such transitions in nuclei up to ^{74}Rb [4,5]. As it is not clear yet how this isospin symmetry-breaking correction should vary with increasing A [6–8], it is important to extend the experimental data set of isospin impurities for nuclei in this mass region.

Various theoretical calculations on isospin mixing for $N = Z$ nuclei have been published, predicting total isospin mixing probabilities ranging from about 1% for ^{56}Ni to about 4% for ^{100}Sn [9–12]. Colò *et al.* [12] have deduced an analytical expression to evaluate the $T = T_0 + 1$ isospin mixing probability P into the $T = T_0$ ground state of $N \approx Z$ nuclei using the energy-weighted sum rule for isovector monopole excitations [13]:

$$P(T = T_0 + 1)$$
$$= \frac{16.09}{(T_0 + 1)} \frac{NZ^3}{A^{7/3}} \left[\frac{1}{E_{\text{IVGMR}} - E_0 + 4V_1(T_0 + 1)/A} \right]^3. \quad (1)$$

Here E_0 is the excitation energy (in MeV) of the state with isospin T_0, E_{IVGMR} represents the energy of the isovector giant monopole resonance which is estimated as $170A^{-1/3}$ MeV in the hydrodynamical model [14], while $V_1 \approx 25$MeV represents a neutron-proton exchange potential [12]. Equation (1) yields predictions for isospin mixing that are close (i.e., within 15–20%) to the results of Hartree-Fock + random phase approximation calculations [12]. As can be seen, isospin mixing becomes smaller when going from the $N = Z$ line to the β-stability line, primarily because of the factor $(T_0 + 1)^{-1}$ (geometrical quenching) and to a lesser extent because of the factor $4V_1(T_0 + 1)/A$ (analog quenching) in the denominator.

Experimental verification of the various theoretical calculations is at present rather limited. Isospin mixing amplitudes can be determined experimentally by searching, e.g., for an $E1$ γ transition between $T = 0$ states or for a Fermi β transition between states with different isospin. Both types of transition are strictly forbidden by isospin conservation. Observation of such transitions therefore indicates mixing between states that differ in isospin but have the same spin and parity.

The first method ($E1$ transitions) is only applicable for $N = Z$ nuclei, while the second one (Fermi β transition) can also be applied when $T \neq 0$, i.e., off the $N = Z$ line. Extracting isospin mixing amplitudes from $E1$ transitions is more difficult because the $E1$ operator is nuclear-structure dependent, as opposed to the Fermi operator, while in addition, one cannot discern in $E1$ transitions whether the mixing occurs in the initial or in the final state. Studying the $E1$ character of the $T = 0$ to $T = 0$, 1665 keV, $5^- \rightarrow 4^+$ γ transition in the $N = Z$ nucleus ^{64}Ge, an isospin mixing probability of 2.4(14)% was found [15]. This mixing amplitude is in reasonable agreement with the estimate of 0.6% from the hydrodynamical model [14] and with the value of 1.2% obtained from Eq. (1).
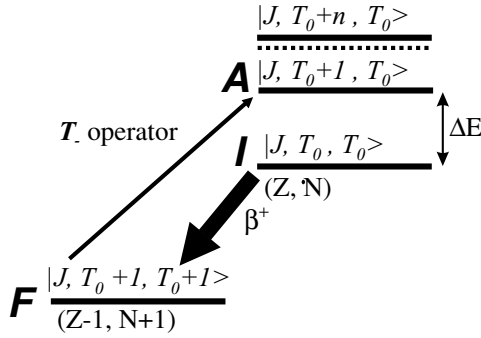
FIG. 1. General decay scheme for an isospin-forbidden β^+ transition with given spin and isospin $|J, T, T_3\rangle$ for the initial I, final F, and analog A levels.

When investigating the presence of isospin-forbidden Fermi β transitions, one probes the admixture amplitude of the analog state A of the final (initial) state into the initial (final) state of a β^+ (β^-) transition (Fig. 1), i.e., the admixture of a specific state only and not the total isospin impurity. Thus, in the case of a β^+ transition, the isospin impurities are present in the initial state; whereas for a β^- transition, isospin impurities are present in the final state.

In a previous paper, we reported already on the isospin impurity in the $T = 1$ ground state of ^{52}Mn. This was deduced from the observed isospin-forbidden Fermi β transition in a measurement of the angular distribution of the ^{52}Mn β^+ particles in a low-temperature nuclear orientation experiment [16]. Here we report on the results of a similar experiment, measuring the isospin impurity in the $J^\pi = 5/2^-$ ground state of ^{71}As, with isospin $T = 5/2$.

II. FORMALISM

We will restrict our work here to the determination of isospin mixing from the experimental observation of an isospin-forbidden Fermi component in β transitions. From the spin and isospin selection rules for allowed Fermi ($\Delta J = 0; \Delta T = 0; \pi_i \pi_f = +$) and Gamow-Teller [$\Delta J = 0, 1$ (not $0 \to 0$); $\Delta T = 0, 1; \pi_i \pi_f = +$] β decay, it follows that the observation of a Fermi component in a $J^\pi \to J^\pi$, $\Delta T = 1$ transition implies isospin mixing, as this Fermi component can only originate from a $\Delta T = 0$ contribution. The formalism for isospin-forbidden $J^\pi \to J^\pi$ Fermi transitions was previously described in detail in [17]. Here we will briefly outline the main parts of it and, moreover, limit our discussion to β^+ transitions with $T_3 \equiv (N - Z)/2 > 0$.

The wave functions of the initial and final state connected by the β^+ transition may be written as (see also Fig. 1)

$$
\begin{aligned}
|i\rangle = {} & |I : J^\pi, T = T_0, T_3 = T_0\rangle \\
& + \alpha |A : J^\pi, T = T_0 + 1, T_3 = T_0\rangle \\
& + \sum_{n>1} \beta_n |J^\pi, T = T_0 + n, T_3 = T_0\rangle,
\end{aligned} \quad (2)
$$

and

$$
\begin{aligned}
|f\rangle = {} & |F : J^\pi, T = T_0 + 1, T_3 = T_0 + 1\rangle \\
& + \sum_{n>1} \beta'_n |J^\pi, T = T_0 + n, T_3 = T_0 + 1\rangle,
\end{aligned} \quad (3)
$$

where as usual $T = T_3$ was used for nuclear ground states and a $T = T_0 + 1$ component (i.e., the analog state A to the final state F) is mixed with small amplitude α into the initial state I. The terms with coefficients β_n and β'_n represent admixtures of states with $T = T_0 + n$ ($n > 1$). Note that α is the admixture coefficient of the analog state A only. Therefore, α^2 does not represent the total isospin impurity of the initial state, but only a fraction of it. The total isospin impurity must be obtained by considering the admixture of all $T \neq T_0$ states into the T_0 state. Possible isospin mixing in the final state is not considered because it can only be of isospin $T_0 + 2$ which cannot be probed by Fermi β decay. To first order in Coulomb mixing amplitudes, the Fermi matrix element is given by

$$
\begin{aligned}
M_F & \equiv \langle f | T^+ | i \rangle = \alpha \sqrt{T^{(A)}(T^{(A)} + 1) - T_3^{(A)}(T_3^{(A)} + 1)} \\
& = \alpha \sqrt{(T_0 + 1)(T_0 + 2) - T_0(T_0 + 1)} \\
& = \alpha \sqrt{2(T_0 + 1)},
\end{aligned} \quad (4)
$$

where the superscript (A) refers to the analog state of the final state. Measuring M_F thus directly yields the isospin mixing amplitude α. Experimentally, this is done by comparing the ft value for the β transition investigated to the nucleus-independent ft value of the superallowed $0^+ \to 0^+$ pure Fermi transitions ($\mathcal{F}t^{0^+ \to 0^+} = 3072.2 \pm 2.0$ s [18]):

$$
ft = \frac{2(G_V)^2 \mathcal{F}t^{0^+ \to 0^+}}{(G_V M_F)^2 + (G_A M_{GT})^2} \quad (5)
$$

and combine this ratio with the Fermi/Gamow-Teller (F/GT) mixing ratio y of the β transition investigated

$$
y = \frac{G_V M_F}{G_A M_{GT}}. \quad (6)
$$

Here G_V (G_A) is the vector (axial-vector) coupling constant and M_F (M_{GT}) is the Fermi (Gamow-Teller) matrix element. Using Eqs. (4)–(6), one then finds for the isospin mixing probability

$$
\alpha^2 = \frac{y^2}{(1 + y^2)(1 + T_0)} \frac{\mathcal{F}t^{0^+ \to 0^+}}{ft}. \quad (7)
$$

Note that the value for $\mathcal{F}t^{0^+ \to 0^+}$ contains a radiative correction, while the ft value for ^{71}As does not. This will yield an error at the few percent level in the deduced value of α^2. This can be neglected, however, since α^2 is only determined at the about 30% accuracy level (see below).

The F/GT mixing ratio y can be extracted from the asymmetry parameter A_1 that is obtained by observing the β^+-emission asymmetry from oriented nuclei:

$$
A_1 = \frac{1}{(1 + y^2)} \left[\frac{-1}{\sqrt{3J(J + 1)}} + \frac{2}{\sqrt{3}} y \right]. \quad (8)
$$

In the work presented here, the nuclei were oriented with the technique of low-temperature nuclear orientation. This method

combines temperatures in the millidegrees Kelvin region with the strong internal magnetic fields that most nuclei feel at substitutional sites in magnetized ferromagnetic host lattices, mostly iron. The sensitivity of this method is illustrated by the fact that, a measurement of e.g., A_1 with an absolute error of ± 0.02 for a β transition from a state with spin $J < 6$ and a log ft value in the range 4.5 to 8 determines α^2 to an absolute precision of better than 10^{-4}, independent of the isospin value of the decaying state.

The angular distribution of positrons emitted in allowed β decay from oriented nuclei is given by [19]

$$W(\Theta) = 1 + f B_1 A_1 \frac{v}{c} Q_1 \cos(\Theta), \qquad (9)$$

where the angle Θ is measured with respect to the magnetic field direction, while v/c is the velocity of the detected positrons relative to the speed of light. Further, Q_1 is a solid angle correction factor that accounts for the geometry of the source-detector arrangement, for positron scattering on the detector surface, and for the influence of the applied magnetic field on the positron trajectories. The coefficient $B_1(T, J, \mu, B_{ext} + B_{hf})$ describes the degree of nuclear orientation of the state with spin J and magnetic moment μ at the temperature T in the orienting magnetic field $B = B_{ext} + B_{hf}$. This field is the sum of the external magnetic field B_{ext} applied to magnetize the iron foil in which the nuclei are implanted and the internal hyperfine magnetic field B_{hf} that the nuclei feel in this foil. Finally, the factor f represents the fraction of nuclei that feel the full orienting hyperfine interaction; whereas in the two-site model, the fraction $(1 - f)$ is supposed to feel no interaction at all. The orientation parameter can be calculated according to the relation

$$B_1 = \sqrt{3(2J+1)} \sum_{m=-J}^{J} (-1)^{J+m} \begin{pmatrix} J & J & 1 \\ -m & m & 0 \end{pmatrix} p_m, \qquad (10)$$

where the p_m describe the population probabilities for the magnetic sublevels with spin projection number m of the state with spin J. For the standard case (i.e., impurity nuclei in thermal equilibrium with the host lattice at a temperature T), the p_m are given by

$$p_m = \exp(m/\Delta_M T) \bigg/ \sum_m \exp(m/\Delta_M T), \qquad (11)$$

where Δ_M is the energy difference between adjacent sublevels (expressed in units of temperature)

$$\Delta_M = \frac{\mu B}{kJ}, \qquad (12)$$

with k the Boltzmann constant.

III. EXPERIMENT

Full details on the decay scheme of $^{71}_{33}$As can be found in [20]. The β^+ transition of interest in this experiment is the allowed $5/2^- \rightarrow 5/2^-$ Gamow-Teller transition with a possible admixture of an isospin- forbidden Fermi component, connecting the ground state of ^{71}As (with isospin $T = T_3 = 5/2$) to the first excited state (with isospin $T = T_3 = 7/2$) at

an excitation energy of 175 keV in the ^{71}Ge daughter isotope. It is the strongest [intensity $I(EC + \beta^+) = (83.20 \pm 0.24)\%$] and most energetic EC/$\beta^+$ transition (endpoint kinetic energy $E_0 = 816$ keV) in the decay of ^{71}As. The second most energetic branch in the β spectrum has an endpoint energy of 793 keV, but as its intensity is only 0.09(8)% of the main one [20], it can be neglected. All other components have β-endpoint energies below 491 keV so that in the energy region from 491 to 816 keV, the spectrum consists of essentially only positrons from the main branch. The reduced half-life (ft) of this main component in the β spectrum is log $ft = 5.85(2)$ [21].

The ground state of ^{71}As (with half-life $t_{1/2} = 65.3$ h) has a magnetic dipole moment $\mu = (+)1.6735(18)$ μ_N, the sign being determined from systematics. The hyperfine magnetic field for As in an iron host lattice is known with good precision and amounts to $B_{hf} = +34.394(27)$ T [22]. The resulting energy splitting between adjacent substates $\Delta_M = \mu B/kJ \simeq 8.4$ mK ensures a reasonable degree of nuclear orientation.

The ^{71}As activity was produced at ISOLDE/CERN. A 5.8 g/cm^2 ZrO$_2$ fiber target [23] was bombarded with 1.0 GeV protons from CERN's proton synchroton booster. The spallation-produced radioisotopes diffuse out of the 1750°C hot target and are subsequently ionized with an unselective ISOLDE-type FEBIAD ion source, accelerated to 60 keV, mass separated at $A/q = 71$, and implanted into a pure Fe foil (99.99%, thickness 100 μm). After being transported to Leuven, all shorter-lived isobars (^{71}Br, ^{71}Se, ^{71}Zn) had decayed and a pure sample of ^{71}As (ca. 40 kBq) and ^{71}Ge remained. The latter emits neither β nor γ particles and hence does not disturb the measurement. The Fe foil was then soldered together with a ^{57}CoFe nuclear thermometer (with an activity of about 25 kBq) on the Cu sample holder of a ^{3}He-^{4}He dilution refrigerator and cooled to millidegrees Kelvin temperatures. A horizontal external magnetic field of $B_{ext} = 0.1$ T, produced by a superconducting split coil magnet and applied parallel to the foil, maintained the magnetization of the sample after it had first been magnetized in a field of 0.4 T. The field was reduced in order to minimize its effect on the trajectories of the β particles.

The β particles were detected with two specially developed windowless HPGe detectors, operating at about 10 K [24] and with a sensitive diameter of about 10 mm and thickness of 3 mm. These were mounted directly on the liquid-helium-cooled shield inside the refrigerator at angles of 14.1° and 162.6° with respect to the magnetic field axis and at a distance of 26 mm from the sample. Both detectors had an energy resolution of about 3.2 keV at 1.33 MeV. The γ rays of the ^{71}AsFe sample and of the ^{57}CoFe nuclear orientation thermometer were observed with two large-volume HPGe detectors. These were placed outside the refrigerator at an angle of 0°, and 90°, respectively, relative to the magnetic field axis and at 73 mm from the sample. Standard electronics, with a precision pulse generator for pile-up and dead-time correction, was used.

The experimental data were collected in two runs. During the first run, about 2000 spectra with an exposure time of 200 s each were recorded. These data were taken as a function of the degree of nuclear orientation by varying the temperature
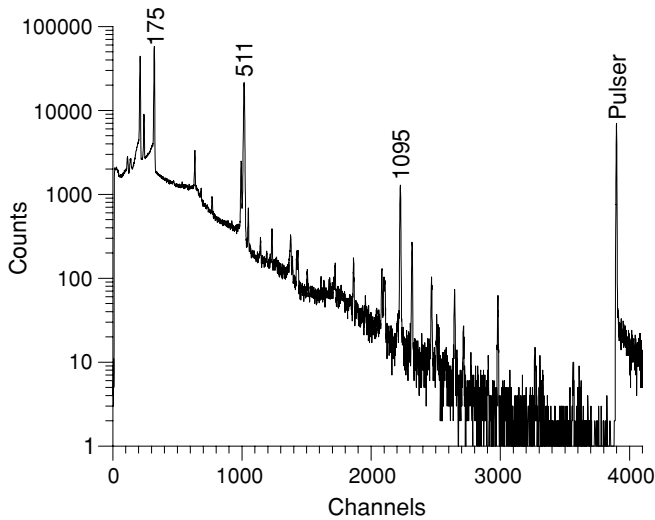
FIG. 2. Warm (i.e., no orientation) γ spectrum of ^{71}As obtained with $0°$ large-volume HPGe detector. Energies of γ lines are in keV.

of the sample. A possible instrumental asymmetry was searched for by reversing the direction of the magnetic field. Figures 2 and 3 show typical unoriented, so-called warm γ and β spectra measured when the sample was at $T \simeq 4.2$ K (at this temperature the ^{71}As and the ^{57}Co nuclei were not oriented). The part of the β spectrum that was used for analysis (see Sec. IV B) is indicated in Fig. 3. It contains about 4.2% of all decays. The time dependence of the number of counts registered by one of the β detectors throughout the entire first run is shown in Fig. 4 for the energy region between 535 and 581 keV. The changes in the number of counts due to the decay of ^{71}As and due to changes in the degree of orientation
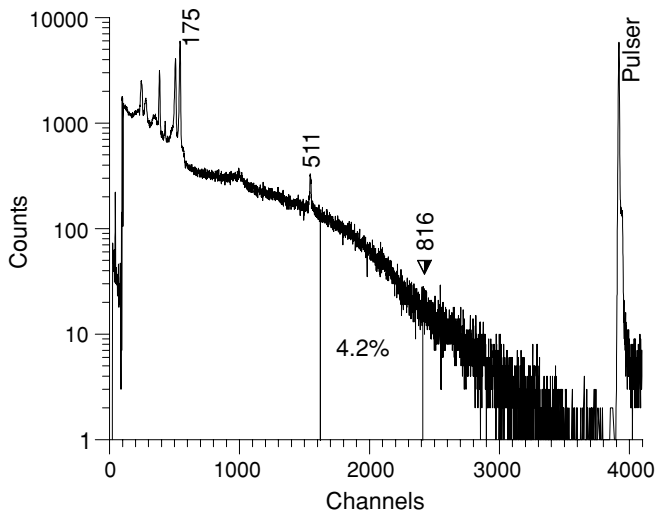

FIG. 3. Warm (i.e., no orientation) β spectrum of ^{71}As obtained with one HPGe particle detector. The 175 and 511 keV γ lines, β-spectrum endpoint at 816 keV, and pulser peak are indicated. Part of the β spectrum used for analysis is region between two vertical lines, containing about 4.2% of total β spectrum. Counts above β-spectrum endpoint are due to Compton γ background and summation effects. Exact procedure is discussed in text.
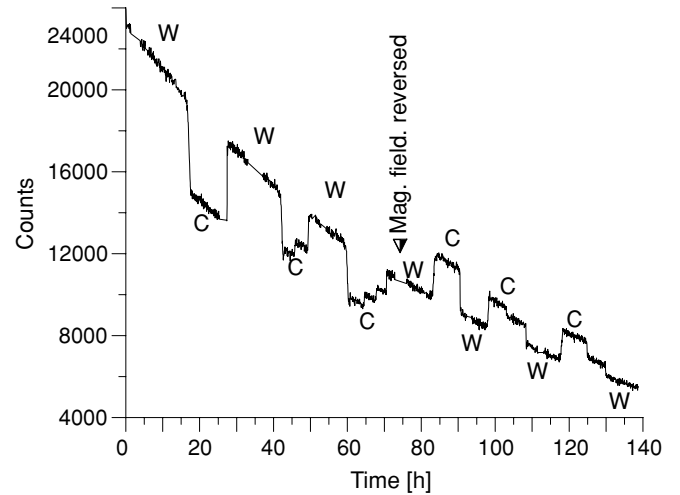

FIG. 4. Counts in 535–581 keV region recorded with one β-particle detector. Data with oriented and unoriented nuclei are indicated by C (cold) and W (warm), respectively. Magnetic field reversal is indicated as well. Decrease of count rate with time reflects ^{71}As half-life.

are clearly visible. Before the second run, the sample was unloaded from the dilution refrigerator and covered with a Ta foil that was sufficiently thick to fully stop all positrons up to the highest energy (i.e., 816 keV). The sample was then loaded again, and about 200 additional spectra with an exposure time of 300 s each were recorded. These spectra were then used to subtract the γ-radiation background in the β-particle detectors. During this second run, the sample was kept at $T \simeq 4.2$ K; i.e., the nuclei were not oriented.

IV. DATA ANALYSIS AND RESULTS

As usual, the experimental angular distribution function $W(\Theta)$ was determined as [19]

$$W(\Theta) = N_{\text{cold}}(\Theta)/N_{\text{warm}}(\Theta), \tag{13}$$

where the quantities $N_{\text{cold}}(\Theta)$ and $N_{\text{warm}}(\Theta)$ are the numbers of counts in a γ peak or a given energy bin in the β spectrum when the sample was cooled to millidegrees Kelvin temperatures (cold) and warmed to about 4.2 K (warm), respectively. The data were corrected for the finite half-life of the ^{71}As nuclei and for the dead time of the detection system. The spectra were corrected for a moderate gain shift before any summing or subtracting of spectra was carried out.

A. γ-ray anisotropies

The experimental anisotropy of the 136 keV γ ray of the ^{57}Co*Fe* sample, measured with the $0°$ HPGe gamma detector, was used to determine the temperature. In the case of γ radiation, the angular distribution function is given by an equation similar to Eq. (9), i.e.,

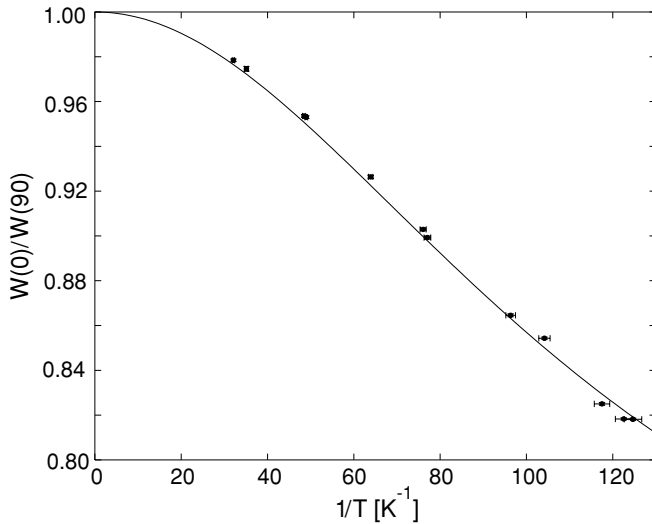$$W(\Theta) = 1 + f \sum_{\lambda=2,4} B_\lambda U_\lambda A_\lambda Q_\lambda P_\lambda \cos(\Theta). \tag{14}$$

FIG. 5. Anisotropy $W(0°)/W(90°)$ versus inverse temperature for 175 keV γ transition in decay of ^{71}As.

The thermometer fraction was determined in a separate experiment as $f_{Co} = 1.00(1)$. The solid angle correction factors Q_2 and Q_4 were determined according to the procedure outlined in [25], adapted for Monte Carlo calculation and duly taking into account the attenuation of the γ rays in the material parts of the dilution refrigerator, including the sample holder and the particle detectors. This yielded for the 136 keV transition, $Q_2 = 0.903(3)$ and $Q_4 = 0.702(9)$. The uncertainties take into account the precision to which the detector geometry was determined, as well as the Monte Carlo statistical error. Because all other parameters that determine the anisotropy of the 136 keV γ line in the decay of ^{57}Co are well known, the temperature could be determined in a unique way from the measured anisotropy and Eq. (14).

For the ^{71}AsFe sample, the fraction f_{As} was obtained by fitting the anisotropy of the strong $5/2^- \rightarrow 1/2^-$ 175 keV γ line in the decay of ^{71}As (Fig. 5) to Eq. (14). The quantities $N_{cold}(\Theta)$ and $N_{warm}(\Theta)$ were corrected for the obvious summing effect of 175 keV γ rays with 511 keV annihilation γ rays. The solid angle correction factors for this transition were calculated to be $Q_2 = 0.893(3)$ and $Q_4 = 0.672(9)$. The fit then resulted in $f_{As}U_2A_2 = -0.2955(40)$, with $\chi^2/\nu = 1.64$ (11 degrees of freedom). On the basis of the ^{71}As decay scheme the U_2 deorientation coefficient for the 175 keV γ ray was calculated to be in the interval [0.6261(42), 0.6675(42)]. In this calculation, the U_2 deorientation coefficient for the β transition that was the subject of this work was needed. Not yet knowing the size of a possible Fermi component in this β transition, we allowed for a Fermi contribution up to about 2%, corresponding to an isospin impurity $\alpha < 0.5\%$ and a F/GT mixing ratio $|y| < 0.14$. This assumption was later confirmed by the analysis (see below). It is to be noted in this respect that since the U_2 deorientation coefficient for a β transition has only a weak dependence on the F/GT mixing ratio, allowing for this small Fermi contribution affected the above-mentioned limits

for U_2 only at the 10^{-3} level while also slightly increasing the error bars. Combining this range of U_2 values with the angular correlation coefficient $A_2(5/2^- \rightarrow 1/2^-) = -0.5345$ for the 175 keV γ transition, one then finds f_{As} to be in the interval [0.828(12), 0.883(13)] or, equivalently, $f_{As} = 0.856(40)$. The $\simeq 10^{-3}$ effect in the values of the U_2 coefficient due to the allowance we made for the isospin impurity in the β transition is thus of no significance at the $\simeq 5\%$ accuracy level obtained for f_{As}.

B. β-particle anisotropies

In determining the β-particle anisotropies, two sources of systematic effects were explicitly taken into account in the data analysis: first, the fact that the particle detectors are sensitive to γ rays, and second, the detector response function.

(i) Besides the strong 175 keV γ line and 511 keV annihilation peak, many weak higher-energy γ lines (together with their continuous Compton distributions) caused a spurious background in the particle detector spectra. For the particle detectors used here, the ratio of absolute efficiencies for the detection of γ and β rays in the energy region from 500 to 900 keV is low, i.e., $\varepsilon(\gamma)/\varepsilon(\beta) < 0.01$. In order to keep the corrections for γ background as low as possible, the region from 535 to 816 keV was selected for the analysis of the β anisotropy, thus avoiding the annihilation radiation line as well as the relatively strong 527 keV γ line in the decay of ^{71}As. The γ spectra measured with the particle detectors in the second run (see above) were first renormalized, taking into account decay, exposure time, and attenuation due to the presence of the Ta foil, and then subtracted from the particle spectra obtained with the same detectors in the main experiment (first run). Table I lists the relative amount of γ background in the six energy bins, each 47 keV wide, used in the analysis of the β spectra. The dependence of this γ background under the β spectra on the degree of nuclear orientation was estimated for each energy bin from the anisotropy that was observed in the corresponding energy regions in the γ spectra recorded with the large HPGe γ detector. The largest γ anisotropy amounted to $N_{cold}/N_{warm} = 1.08$ only. This effect was included in the statistical error when subtracting the γ background from the β spectra.

(ii) The β spectrum measured with a HPGe detector is distorted from its ideal shape. It is assumed that distortions due to backscattering, sidescattering, and summing of the β signal with annihilation radiation are included in the detector response function. We adopted the semiempirical detector response function described by Rehfield and Moore [26] for the region above 511 keV (Fig. 6). This response function is composed of four fractions with areas bs, mainly backscattering; fp, full energy peak; as, annihilation Compton summing tail; and ap, 511 keV annihilation summing peak. The double-summing region mentioned in [26] which extends above the 511 keV annihilation summing peak was negligible in our case because the particle detectors were rather thin. The ratios bs:fp:as:ap can reasonably be assumed to be independent of energy over the limited energy range considered in this analysis. The shapes of the β spectra for warm (nonoriented) and cold (oriented)

TABLE I. Relative γ background in β spectrum as a function of energy, in region from 535 to 816 keV.

Bin	1	2	3	4	5	6
Energy region (keV)	535–581	582–628	629–675	676–722	723–769	770–816
$\gamma/(\beta+\gamma)$ (%)	2.5	2.8	3.2	4.2	5.4	9.1

conditions are then given by the convolutions

$$N_{\text{warm}}(\Theta, E) = C \int_0^{E_{\max}} S(E', E) dE', \tag{15}$$

$$N_{\text{cold}}(\Theta, E) = C \int_0^{E_{\max}} S(E', E) \\ \times \left[1 + f B_1 Q_1 \frac{v(E')}{c} A_1 \cos(\Theta) \right] dE', \tag{16}$$

with

$$S(E', E) = \lambda(E', E_{\max}, Z) R(E', E, \Theta), \tag{17}$$

and where C is a constant, $\lambda(E', E_{\max}, Z)$ is the theoretical shape of the allowed β spectrum, and $R(E', E, \Theta)$ is the response function of the β-particle detector at angle Θ. Constructing from the experimental data the ratio

$$\widetilde{W}(\Theta, E) = N_{\text{cold}}(\Theta, E)/N_{\text{warm}}(\Theta, E) \tag{18}$$

and using Eqs. (15)–(17), one derives

$$f A_1 = \frac{\widetilde{W}(\Theta, E) - 1}{B_1 Q_1 \cos(\Theta) f^{\text{cor}}(\Theta, E)}, \tag{19}$$

the correction function $f^{\text{cor}}(\Theta, E)$ being given by

$$f^{\text{cor}}(\Theta, E) = \frac{\int_0^{E_{\max}} S(E', E) \frac{v(E')}{c} dE'}{\int_0^{E_{\max}} S(E', E) dE'}. \tag{20}$$
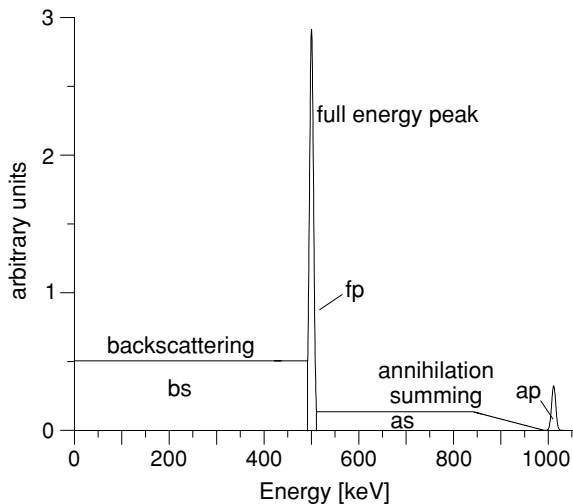
When two particle detectors at angles Θ_1 and Θ_2 are used, the following double ratio can be constructed

$$\widetilde{W}'(E) = \frac{N_{\text{cold}}(\Theta_1, E)/N_{\text{warm}}(\Theta_1, E)}{N_{\text{cold}}(\Theta_2, E)/N_{\text{warm}}(\Theta_2, E)}. \tag{21}$$

In this case, one has instead of Eq. (19)

$$f A_1 = \frac{1 - \widetilde{W}'(E)}{\widetilde{W}'(E) D_2 - D_1}, \tag{22}$$

$$D_i = (B_1 Q_1)_i \cos(\Theta_i) f^{\text{cor}}(\Theta_i, E), \tag{23}$$

with $(i = 1, 2)$.

The detection angles Θ_i for the β detectors were measured to be (for both directions of the magnetic field) $\Theta_1 = 14.1(10)°$ or $165.9(10)°$, $\Theta_2 = 17.4(10)°$ or $162.6(10)°$. Using a Monte Carlo program that takes into account the influence of the magnetic field (0.1 T) on the β-particle trajectories as well as scattering on the detector surface, the solid angle correction factors $Q_1(\Theta_1) = 0.983(20)$ and $Q_1(\Theta_2) = 0.982(20)$ were then obtained. Figure 7 shows the temperature dependence of $\widetilde{W}(14.1°)$ and $\widetilde{W}(162.6°)$ for part of the data, for the energy bin from 676 to 722 keV.

The parameters fp, bs, ap, and as of the response functions for both particle detectors were determined by fitting the relevant warm spectra in the energy interval 535–1000 keV. Then, Eqs. (19) or (22) were used to determine the parameter $f A_1$ in the six energy bins defined above and for the 12 temperatures (i.e., degrees of orientation). The weighted averaged results that were thus obtained for the parameter $f A_1$ for each of the six energy bins are displayed in Fig. 8. When the detector response function $R(E', E, \Theta)$ was not taken into
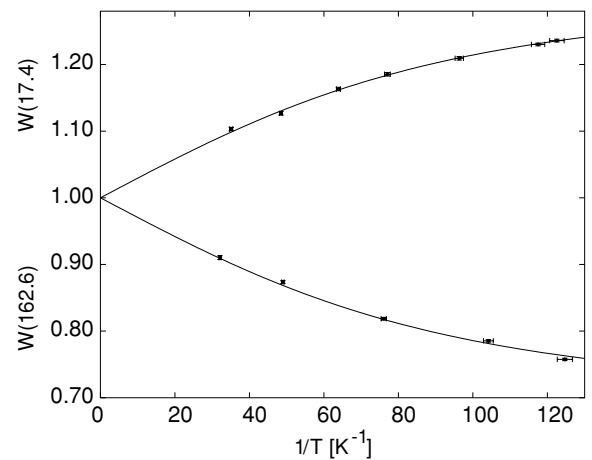

FIG. 6. Semiempirical response function for a 500 keV positron recorded with a HPGe detector.

FIG. 7. Temperature dependence of β anisotropy for energy bin from 676 to 722 keV, observed with one particle detector for both directions of the external magnetic field and for part of the data.
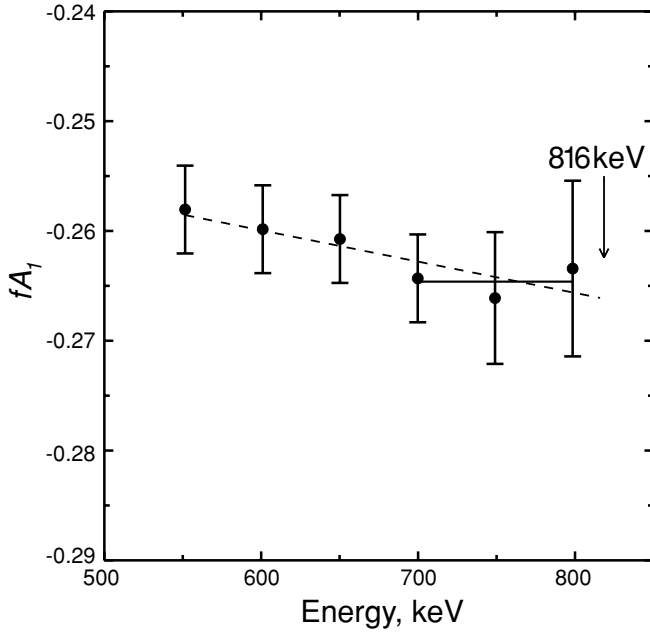
FIG. 8. Values for fA_1 for six energy bins. Decrease of absolute value of fA_1 toward lower energies is due to scattering effects. Dashed line, fit of a straight line to data points. Full line, fit of a constant to three highest energy points. Error bars indicate statistical errors only.

TABLE II. Total error account for fA_1, including statistical error and different systematic errors related to fitting procedure and to error bars for B_1, for different Q_1 values, and for detection angles Θ. Because the value and error for B_1 are different for each of the 12 temperature points, we conservatively used the maximal value for error on the 12 B_1 values to calculate the corresponding contribution to the systematic error.

Source	Statistics	Fit	B_1	Q_1	Θ	Total
Error	0.0022	0.0028	0.0017	0.0039	0.0010	0.0056

However, effects of scattering should become smaller and finally disappear toward the β-endpoint energy. We therefore fitted at first a straight line to the set of six fA_1 values, yielding $fA_1 = -0.2675(22)$ for the spectrum endpoint (i.e., 816 keV). next, a constant was fitted through the three highest energy points, which do not show any trend for a slope, yielding $fA_1 = -0.2647(13)$, in good agreement with the result from the first fit. As it is not clear which of these two approaches is to be preferred, we decided to adopt the first value, which is based on all data points, and to use the difference between the two fit results as a systematic error caused by the "fitting procedure." The total systematic error account is given in Table II. Adding the statistical and systematic errors in quadrature then yields $fA_1 = -0.267(6)$. Combining this now with the value for the fraction $f = 0.856(40)$ that was obtained from the anisotropy for the 175 keV γ ray, one finally gets for the β-asymmetry parameter $A_1 = -0.312(16)$.

This result for A_1 corresponds to a F/GT mixing ratio of either $y = -0.104(15)$ or $y = -3.60(20)$. The last value can be discarded as this would correspond to a Fermi contribution of about 93%; whereas this decay should have pure Gamow-Teller character according to the isospin selection rule, and any isospin impurity is expected to induce only a small Fermi contribution. The mixing ratio $y = -0.104(15)$ corresponds to a Fermi contribution of 1.1(3)%. Combining this mixing ratio with the logft value of 5.85(2) and using Eqs. (7) and (4), the isospin mixing amplitude and the corresponding Fermi matrix element are found to be $|\alpha| = 3.64(55) \times 10^{-3}$ and $|M_F| = 9.6(15) \times 10^{-3}$. One then finally gets for the charge-dependent nuclear matrix element $|\langle V_{CD}\rangle| = \Delta E |\alpha| = 28(4)$ keV, with $\Delta E = 7.58(6)$ MeV [17] being the energy difference between the admixed state [i.e., the analog state of the daughter state; Fig. (1)] and the ground state of ^{71}As.

account, the absolute values obtained for fA_1 were smaller by only 0.01, corresponding to a relative change of about 3.5%. This small influence of the detector response function is due to the relative character of our measurements; i.e., fA_1 is extracted from the ratio of counts in the cold and warm spectra [Eqs. (19) and (22)] that are, to first order, influenced in the same way by the response function. In calculating the data for fA_1, the sign of the magnetic moment μ of ^{71}As was taken to be positive (from systematics). Negative values for fA_1 were then obtained. This agrees with the fact that the sign of A_1 must be negative for a $J^\pi \rightarrow J^\pi$ β^+ transition with small absolute value of the F/GT mixing ratio y. Indeed, in the case of a pure Gamow-Teller transition, i.e., in the absence of any isospin mixing, $A_1 = -0.195$ is expected for a $5/2^- \rightarrow 5/2^-$ β^+ transition, while for not-too-large isospin impurities (i.e., $\alpha < 0.5\%$, corresponding to $|y| < 0.14$ in the case of ^{71}As), the value for A_1 remains negative; viz, $A_1 = -0.03$ for $y = +0.14$ and $A_1 = -0.35$ for $y = -0.14$. Isospin impurities α larger than 0.5% were observed for only two β transitions until now [17]. That a value for $|y|$ smaller than 0.14 was indeed obtained in our experiment (see below) confirms the positive sign for the magnetic moment of ^{71}As.

As can be seen from Fig. 8, there seems to be a small trend in the data points indicating a systematic decrease of $|fA_1|$ toward lower energies. This is probably due to scattering of the positrons in the Fe host foil and its backing. Indeed, although the effect of scattering is taken into account in the response function, a small effect can still remain because the parameters of the response function were fitted from the warm (isotropic) spectra, while they will be slightly different for the cold spectra, when the positrons are emitted anisotropically.

V. CONCLUSION

A small isospin-forbidden Fermi component [$|M_F| = 9.6(15) \times 10^{-3}$] was observed in the $5/2^- \rightarrow 5/2^-$ β^+ transition of the $5/2^-$, $T = 5/2$ ground state of ^{71}As to the $5/2^-$, $T = 7/2$ first excited state of ^{71}Ge, corresponding to an isospin mixing probability $\alpha^2 = 13(4) \times 10^{-6}$ in the ^{71}As ground state. The smallness of this isospin mixing probability and the corresponding change of the A_1 β asymmetry parameter from a value of -0.195 in the absence of isospin mixing to the observed value of $-0.312(16)$ illustrate the high sensitivity of the method used here for detecting isospin

impurities. The observed isospin admixture is similar to the one previously obtained for the 6^+, $T = 1$ ground state of ^{52}Mn [16], i.e., $\alpha^2 = 7(3) \times 10^{-6}$. Furthermore, our result is about three orders of magnitude smaller than the value of $P = 0.0031$ obtained from Eq. (1) for the total isospin mixing probability of states with $T = T_0 + 1$ into the $T_0 = 5/2$ ground state of ^{71}As. It is to be noted, however, that our result does not correspond to the total isospin impurity in the ^{71}As ground state but only to the isospin admixture from the analog state of the final state of the β transition observed, i.e., the analog state of

the $5/2^-$, $T = 7/2$ first excited state of ^{71}Ge. This analog state thus contributes only about 0.5% of the total $T_0 + 1$ isospin impurity in the ground state of ^{71}As.

[1] R. Schneider *et al.*, Z. Phys. A **348**, 241 (1994).

[2] M. Lewitowicz *et al.*, Phys. Lett. **B332**, 20 (1994).

[3] T. Faestermann *et al.*, Eur. Phys. J. **15**, 185 (2002).

[4] J. C. Hardy and I. S. Towner, Phys. Rev. Lett. **94**, 092502 (2005).

[5] A. Kellerbauer *et al.*, Phys. Rev. Lett. **93**, 072502 (2004).

[6] W. E. Ormand and B. A. Brown, Phys. Rev. C **52**, 2455 (1995).

[7] H. Sagawa, N. Van Giai, and T. Suzuki, Phys. Rev. C **53**, 2163 (1996).

[8] I. S. Towner and J. C. Hardy, Phys. Rev. C **66**, 035501 (2002).

[9] I. Hamamoto and H. Sagawa, Phys. Rev. C **48**, R960 (1993).

[10] J. Dobaczewski and I. Hamamoto, Phys. Lett. **B345**, 181 (1995).

[11] H. Sagawa, Nguyen Van Giai, and T. Suzuki, Phys. Lett. **B353**, 7 (1995).

[12] G. Colò, M. A. Nagarajan, P. Van Isacker, and A. Vitturi, Phys. Rev. C **52**, 1175(R) (1995).

[13] E. Lipparini and S. Stringari, Phys. Rep. **175**, 103 (1989).

[14] A. Bohr and B. A. Mottelson, in *Nuclear Structure*, (Benjamin, New York, 1969), Vol. **1**.

[15] G. de Angelis *et al.*, in *Proceeding of the 3rd International Conference on Exotic Nuclei and Atomic Masses*, ENAM2001

(Hämeenlinna, Finland, 2–7 July 2001), edited by J. Äystö, P. Dendooven, A. Jokinen, and M. Leino (Springer, Berlin, 2003), p. 277.

[16] P. Schuurmans, J. Camps, T. Phalet, N. Severijns, B. Vereecke, and S. Versyck, Nucl. Phys. **A672**, 89 (2000).

[17] S. Raman, T. A. Walkiewicz, and H. Behrens, At. Data Nucl. Data Tables **16**, 451 (1975).

[18] I. S. Towner and J. C. Hardy, J. Phys. G: Nucl. Part. Phys. **29**, 197 (2003).

[19] K. S. Krane in *Low-Temperature Nuclear Orientation*, edited by N. J. Stone and H. Postma (North-Holland, Amsterdam, 1986), Chap. 2.

[20] M. R. Bhat, Nucl. Data Sheets **68**, 579 (1993).

[21] H. Junde, Nucl. Data Sheets **90**, 1 (2000).

[22] G. N. Rao, Hyperfine Interact. **24-26**, 1119 (1985).

[23] U. Köster *et al.*, Nucl. Instrum. Methods B **204**, 303 (2003).

[24] D. Vénos, A. Van Geert, N. Severijns, D. Srnka, and D. Zakoućky, Nucl. Instrum. Methods A **454**, 403 (2000).

[25] K. S. Krane, Nucl. Instrum. Methods **98**, 205 (1972).

[26] D. M. Rehfield and R. B. Moore, Nucl. Instrum. Methods **157**, 365 (1978).